Dynamic power balance for nonlinear waves in unbalanced gain and loss landscapes

Yannis Kominis
School of Applied Mathematical and Physical Science, National Technical University of Athens, Zographou GR-15773, Greece
(Received 19 August 2015; published 30 December 2015)

The presence of losses in nonlinear photonic structures necessitates the introduction of active parts for wave power compensation resulting in unbalanced gain and loss landscapes where localized beam propagation is, in general, dynamically unstable. Here we provide generic sufficient conditions for the relation between the gain-loss and the refractive index profiles in order to ensure efficient wave trapping and stable propagation for a wide range of beam launching conditions such as initial power, angle of incidence, and position. The stability is a consequence of an underlying dynamic power balance mechanism related to a conserved quantity of wave dynamics.

DOI: 10.1103/PhysRevA.92.063849 PACS number(s): 42.65.Tg, 42.65.Jx, 42.65.Sf, 78.67.Pt

Modern photonic applications utilize the combination of nonlinearity and inhomogeneity in order to provide advanced functionality in properly engineered metamaterials and metadevices [1,2]. These structures have the form of multilayered media consisting of materials such as ordinary dielectrics as well as metals and graphene. The presence of metals results in plasmonic excitations that can boost nonlinear effects due to high field values and small mode volume [3], whereas the presence of graphene layers is accompanied by very strong Kerr nonlinearities [4], both resulting in the formation of self-localized modes [5–8]. The nonlinearity plays a crucial role in functionality related to dynamic and all-optical light control through wave-material and wave-wave interactions. However, both ordinary dielectrics and metal or graphene layers introduce significant losses that can hamper the nonlinear functionality of these structures by restricting the wave propagation to small distances [9]. This crucial drawback of the respective photonic structures necessitates the utilization of active parts (hot spots) in the form of doped and pumped dielectrics in order to provide the necessary gain for loss compensation [10–12], introducing an inhomogeneous gain-loss landscape. A similar type of nonconservative inhomogeneity also appears in applications related to soliton-forming laser cavities [13]. In all these cases the formation and robust propagation of a self-localized mode is determined by both the diffraction-nonlinearity and the loss-gain balance, which cannot be considered separately.

From an engineering aspect, even the presence of spatially homogeneous gain and loss in an optical lattice can significantly enrich soliton dynamics providing soliton routing and acceleration functionalities [14,15], in addition to the numerous applications related to conservative lattices that include the formation of solitons, surface waves, and defect modes [16,17]. Moreover, the appropriate design of gain and loss inhomogeneity provides another degree of freedom for wave manipulation [18,19]. The symmetry properties of the inhomogeneity profiles have been shown to play a crucial role in the system features. It has been shown that, for the case of $\mathcal{PT}$ symmetry, the system has a real spectrum and supports a continuous family of solitons [20,21]. Other types of symmetries that restrict, not the profiles of the refractive index and the gain-loss inhomogeneity as in the $\mathcal{PT}$ case, but their mutual relation, have also been shown to support such continuous soliton families [19,22,23], in contrast to the common case of dissipative solitons in which, in general, only isolated solitons exist.

A solitary wave can propagate at a fixed transverse position of a planar structure near the interface between a gain and a loss region, where a static power balance condition is satisfied. However, any deviation from this specific position or from a zero angle of incidence can lead to continuous power increasing or decreasing, resulting in unstable behavior, as in the case of stationary solitons pinned to hot spots [24–30]. The utilization of spatial modulations of the linear or nonlinear refractive index has been proposed [31,32] for introducing effective potential wells resulting in wave trapping in the specific position and preventing large excursions within the two regions around the fixed position. Even in such cases, wave oscillations around the balance position can be unstable when the gain and loss of the interfaced parts are unbalanced, as in the most typical case in which narrow hot spots with high gain are utilized in order to compensate for more extended parts with relatively small losses. The instability arises from the fact that the dynamic power balance of the wave depends on the extent of the oscillations in the two parts, since the wave amplification and attenuation in the two phases of the oscillation are not equal in general. Therefore, an appropriate refractive index modulation has to take into account the gain and loss profile in order to ensure a dynamic balance of gain and loss and a stable wave propagation.

In the following, we present generic efficient conditions for the relation between the gain-loss and the refractive index profiles allowing not only for stable stationary propagation at a specific point with a zero angle of incidence, but also for dynamic power balance for localized waves with a wide range of positions and angles of incidence, which are applicable to any type of planar photonic structure that may have unbalanced gain and loss properties.

I. MODEL AND METHOD

Nonlinear wave propagation in a transversely inhomogeneous planar photonic structure is described by the nonlinear Schrödinger equation (NLSE)

$$iu_z + u_{xx} + [V(x) - iW(x)]u + 2|u|^2u = 0, \qquad (1)$$

where u is the normalized electric field envelope, z and x are the normalized longitudinal and transverse dimensions, and $V(x)$, $W(x)$ are the transverse refractive index and gain-loss profiles, respectively. For spatially localized (solitary) waves, neglecting radiation losses, we can define the useful quantities corresponding to the wave mass $m = \int |u|^2 dx$ and momentum $p = i \int (u u_x^* - u_x u^*) dx$. In the absence of inhomogeneity ($V = W = 0$), m and p are conserved, whereas in the presence of inhomogeneity they vary as

$$\frac{dm}{dz} = \Gamma(x_0), \tag{2}$$

$$m\frac{dv}{dz} = -\frac{\partial U_{\text{eff}}(x_0)}{\partial x_0}, \tag{3}$$

where

$$\Gamma(x_0) = 2\int_{-\infty}^{+\infty} |u(x - x_0)|^2 W(x) dx, \tag{4}$$

$$U_{\text{eff}}(x_0) = -2\int_{-\infty}^{+\infty} |u(x - x_0)|^2 V(x) dx \tag{5}$$

are the mass variation rate and the effective potential, respectively, and x_0 is the wave center varying as $dx_0/dz = p/m \equiv v$ with the velocity v corresponding to the propagation angle. Therefore, the solitary wave propagates as an effective particle with mass and momentum variations depending on the nonconservative $[W(x)]$ and the conservative $[V(x)]$ part of the inhomogeneity, respectively. Wave propagation dynamics are described in the three-dimensional space (x_0, v, m). By dividing Eqs. (2) and (3) and changing the integration variable from x to $x - x_0$ in Eqs. (4) and (5), it can be readily shown [19] that, under the condition

$$\frac{\partial V(x)}{\partial x} = C W(x), \tag{6}$$

the existence of an exact invariant of the motion, given by $K = C \ln m + v$, restricts the wave dynamics in a two-dimensional surface. This is a general property of any type of solitary wave in the presence of inhomogeneities of arbitrary profile and magnitude. Condition (6) ensures the static power balance for a stationary solitary wave located at a fixed point $\Gamma(x_0) = 0$ in the vicinity of the interface between a lossy and an amplifying part. Moreover, it is a stronger condition, sufficient for the dynamic power balance of solitary waves with nonzero angles of incidence and positions deviating from the fixed point that undergo stable oscillations, as we show in the following. Notice that condition (6) is qualitatively different from the $\mathcal{PT}$ symmetry condition, since it does not imply any restriction on the symmetry properties of the nonconservative $[W(x)]$ and the conservative $[V(x)]$ part of the inhomogeneity, but only a mutual relation of their profiles; therefore, it is also applied in nonsymmetric profiles. Under condition (6) when $V(x)$ is even, $W(x)$ is odd (and vice versa) as in $\mathcal{PT}$ symmetric configurations. However, the $\mathcal{PT}$ symmetry condition suggests only the existence of a fixed point and does not ensure its stability.

In the following, we exploit the consequences of this condition with respect to the dynamic power balance for solitary waves in a wide variety of planar structures, and we prove that Eq. (6) serves as a generic sufficient condition for stable wave propagation in accordingly designed photonic structures.

II. RESULTS AND DISCUSSION

We focus on multilayer photonic structures with piecewise constant gain and loss profiles. According to Eq. (6), the linear refractive index profile is a piecewise linear function, so that

$$W(x) = \sum_i \Pi_i(x), \qquad V(x) = \sum_i \Lambda_i(x) \tag{7}$$

with

$$\Pi_i(x) = \begin{cases} a_i, & x_{i,1} < x < x_{i,2}, \\ 0 & \text{elsewhere}, \end{cases} \tag{8}$$

$$\Lambda_i(x) = \begin{cases} c_i x + d_i, & x_{i,1} < x < x_{i,2}, \\ 0 & \text{elsewhere}. \end{cases} \tag{9}$$

The dynamics of solitary wave propagation in such structures is determined by Eqs. (2) and (3). To simplify our analysis and provide an intuitive understanding, we consider inhomogeneities of relatively small amplitude. According to a perturbative approach, we assume that the solitary wave form remains close to the soliton solution of the homogeneous NLSE $u = \eta\,\text{sech}[\eta(x - x_0)]\exp[i(v/2)x + i(\eta^2 - v^2/4)z]$ that is utilized in order to obtain the integrals appearing in Eqs. (4) and (5) in closed form,

$$\Gamma(x_0) = m\sum_i [\pi_i(x_{i,2}) - \pi_i(x_{i,1})], \tag{10}$$

$$U_{\text{eff}}(x_0) = -2m\sum_i [\lambda_i(x_{i,2}) - \lambda_i(x_{i,1})], \tag{11}$$

$$\pi_i(x) = a_i \tanh\frac{m}{2}(x - x_0), \tag{12}$$

$$\lambda_i(x) = c_i(x - x_0) - \frac{c_i x + d_i}{e^{m(x-x_0)} + 1} - \frac{c_i}{m}\ln(e^{m(x-x_0)} + 1) \tag{13}$$

with $m = 2\eta$.

First, we consider a structure consisting of two interfaced semi-infinite parts with unequal gain and loss coefficients and linear refractive indices profiles fulfilling condition (6) with $C = -1$ as shown in Fig. 1(a). The effective potential has a local minimum, corresponding to a fixed point, in the vicinity of the interface with its exact position depending on the soliton mass. For a soliton of mass $m = 1$, the fixed point is located at $x_0 = -0.69$. Stable propagation of a stationary soliton with initial position at the fixed point is shown in Fig. 1(b). The fulfillment of condition (6) results in refractive index slopes appropriately defined in terms of the gain and loss coefficients in each part. In terms of soliton dynamics, the direct consequence of the condition is that the trapping potential is such that no continuous mass increase or decrease takes place, as the traveling distance in each region is such that the soliton spends less time in the high-gain region than in the low-loss region. In fact, this dynamic power balance mechanism results in asymptotic evolution to the stable fixed point (attractor). As shown in Fig. 1(c), the effective particle orbit for a soliton initially located at $x_0 = -10$ evolves to the fixed point while remaining in the aforementioned two-dimensional surface of the phase space.

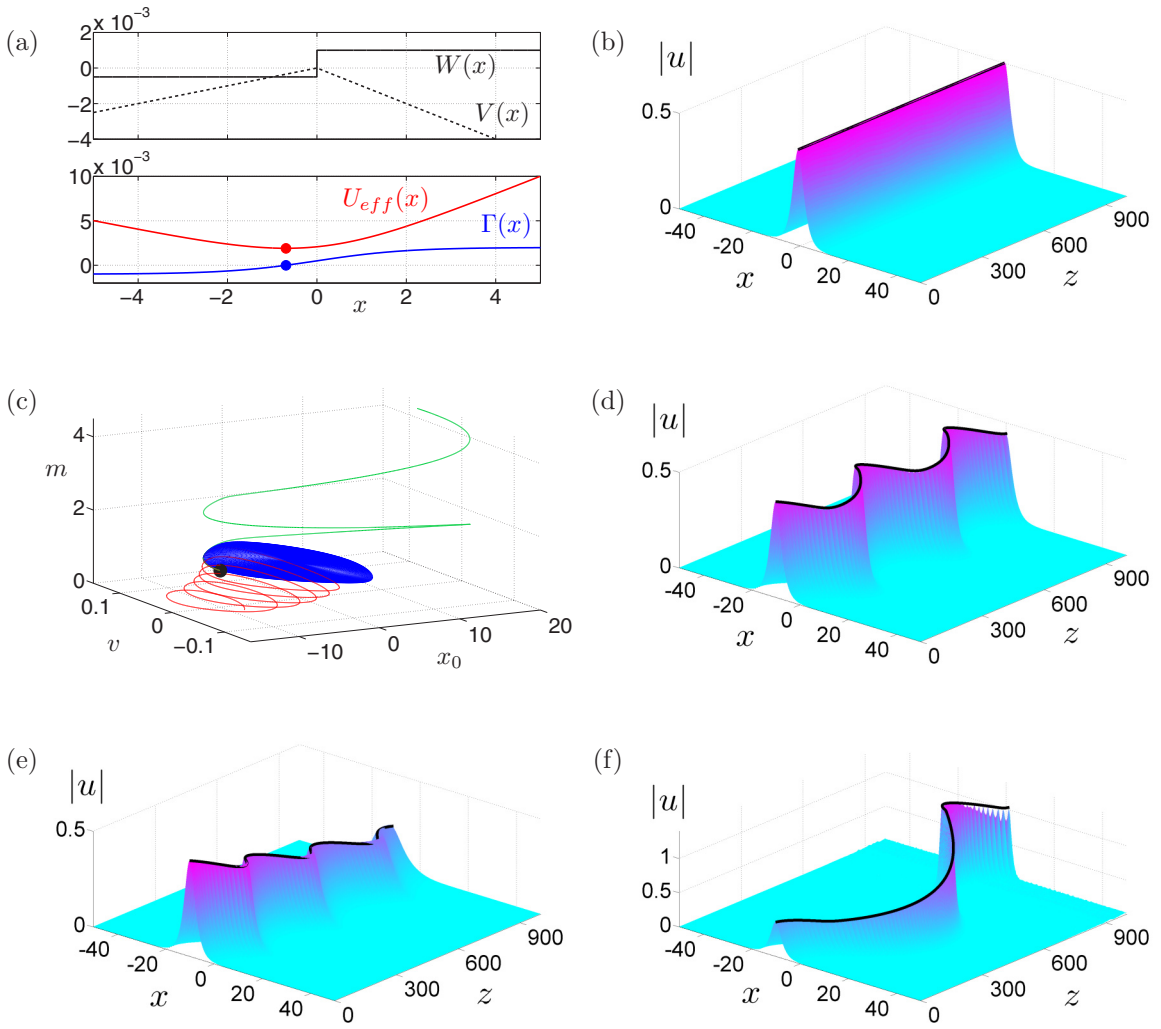

FIG. 1. (Color online) Single interface between a lossy ($a_1 = -0.0005$) and an amplifying ($a_2 = 0.001$) region. (a) Gain-loss $W(x)$ and refractive index $V(x)$ profiles (top); effective potential $U_{\text{eff}}(x_0)$ and mass variation rate $\Gamma(x_0)$ for a soliton of mass $m = 1$ for a refractive index profile fulfilling the condition (6) with $C = -1$ ($c_i = -a_i, i = 1,2$) (bottom). (b) Stationary propagation for initial soliton position $x_0 = -0.69$ corresponding to the fixed point depicted by a thick dot in (a). (c) Phase-space orbits of a soliton with initial position $x_0 = -10$ under dynamic balance conditions $c_i = -a_i, i = 1,2$ (blue), and for unbalanced cases with $c_1 = -a_1, c_2 = -7a_2$ (red), $c_1 = -a_1, c_2 = -0.25a_2$ (green). (d),(e),(f) Soliton propagation for conditions corresponding to the three orbits shown in (c). The thick black lines depict results from the effective particle model.

The rate of convergence to the fixed point orbit increases with the magnitude difference between the gain and loss coefficients, and for the specific case it is quite small, as shown in Fig. 1(d). Notice that the period of oscillations scales with $|C|^{-1/2}$. Within the effective particle approach, it is obvious that the propagation of a soliton with a given initial mass is determined by its initial position and velocity. In fact, it is the sum of the "kinetic" and the "potential" energy of the effective particle and its relation with the potential energy landscape that determines whether a soliton remains trapped or not. Therefore, nonzero initial velocities result in soliton trapping if the aforementioned sum is smaller than the effective potential energy maxima forming a potential barrier. In the case of Fig. 1(a), where the effective potential continuously increases with the distance from the interface, soliton trapping always occurs, under condition (6), whereas other configurations in the presence of finite local maxima of the effective potential result in solitons traveling across the structure, as shown in the following. The importance of condition (6) can be shown in comparison to the cases in which it is not fulfilled, resulting in continuous mass either decreasing or increasing, as shown in Figs. 1(e) and 1(f), respectively, and unbounded phase-space orbits [Fig. 1(c)].

A typical realistic case with practical importance is a planar structure consisting of an amplifying part of finite width (hot spot) in a lossy medium, with gain-loss and refractive index profiles fulfilling condition (6), as shown in Fig. 2(a). For a soliton of mass $m = 1$ and the parameters values of the specific structure, an asymmetric potential well can be formed, as shown in Fig. 2(a). The fixed point located at $x_0 = -2.65$ corresponds to stable stationary soliton propagation [Fig. 2(b)], whereas stable large-amplitude oscillations (asymptotically evolving to the stationary soliton) can take place as a consequence of the condition for dynamic power balance, as

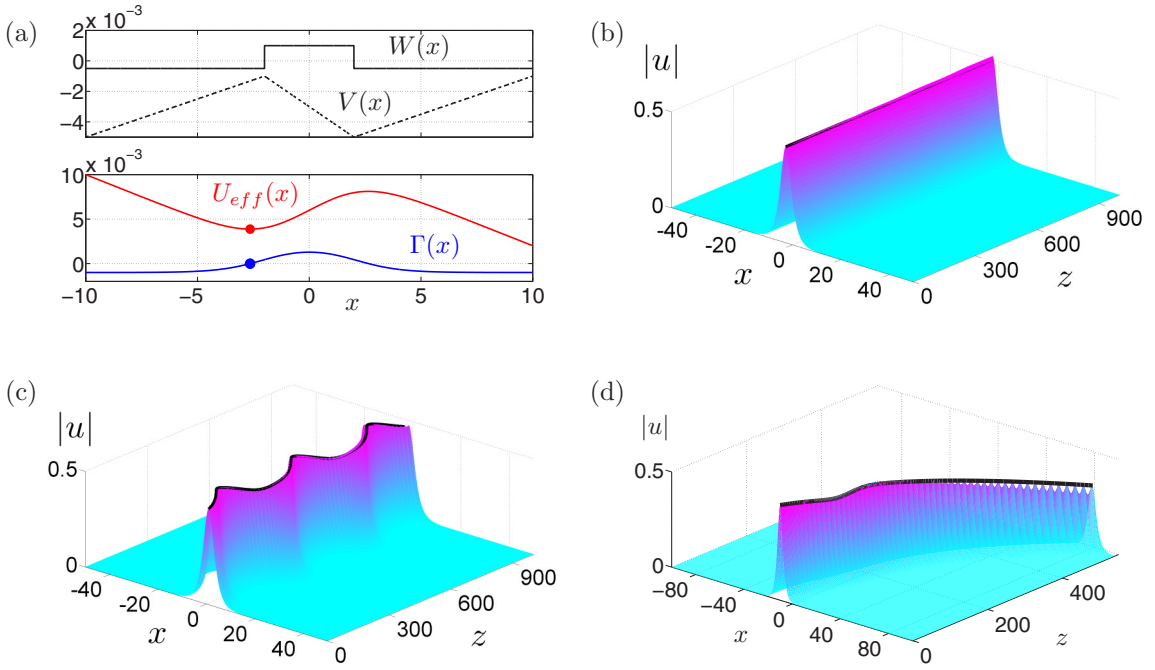

FIG. 2. (Color online) Single hot-spot structure consisted of an amplifying part ($a_2 = 0.001$) of finite width $\Delta x = 4$ in a lossy medium ($a_1 = a_3 = -0.0005$) for a refractive index profile fulfilling the condition (6) with $C = -1$ ($c_i = -a_i, i = 1,2$). (a) Gain-loss $W(x)$ and refractive index $V(x)$ profiles (top); effective potential $U_{\text{eff}}(x_0)$ and mass variation rate $\Gamma(x_0)$ for a soliton of mass $m = 1$ (bottom). (b) Stationary propagation for initial soliton position $x_0 = -2.65$ corresponding to the fixed point depicted by a thick dot in (a). (c) Trapped soliton oscillations for initial position $x_0 = 1$. (d) Traveling soliton propagation for initial position $x_0 = -10$. The thick black lines depict results from the effective particle model.

shown in Fig. 2(c). Since the potential well does not have an infinite depth, initial soliton conditions corresponding to untrapped dynamics result in traveling solitons of continuously decreasing mass, as illustrated in Fig. 2(d). It is worth noting that the trapping conditions depend on both the parameters of the structure and the soliton mass, so that in each structure solitons having a mass below a critical value cannot be trapped. This fact results from the interplay of the two spatial scales, namely the soliton width ($\sim m^{-1}$) and the amplifying part width (Δx) as well as the relative magnitude of the gain and loss coefficients, and it is reflected in the effective particle model as a bifurcation of the fixed point corresponding to the local minimum of the effective potential. The spatial width and the depth of the potential well, for a given soliton mass value, determine the range of initial positions and angles of incidence (velocities) for soliton trapping and stability.

The case of a structure with two hot spots is considered in Fig. 3. As expected, the increased complexity of the structure results in richer dynamics and trapping capabilities. In such a case we can have two fixed points, as shown Fig. 3(a). Therefore, under dynamic power balance conditions, trapping and stable soliton oscillations can occur either on the left potential well [Fig. 3(b)] or on the right one [Fig. 3(c)]. Moreover, for appropriate initial conditions, extended stable oscillations can take place in the region above the two potential wells for effective particle energy above the left and below the right local maximum of the effective potential [Fig. 3(d)]. The existence and bifurcations of the two fixed points again depend on the soliton mass and the parameters of the structure, so that we can have two, one, or zero fixed points for a given soliton mass value.

The robust coexistence of two solitons trapped in the two different potential wells is illustrated in Fig. 4(a) for soliton mass $m = 1$. Although initially located at the corresponding fixed points, solitons oscillate due to mutual interactions depending strongly both on the soliton width (mass) and the distance between the two hot spots. Different interaction scenarios are possible, as in the case of two solitons of higher mass ($m = 1.5$) as shown in Fig. 4(b). In that case, although both solitons are launched at the corresponding fixed points, under interaction the right one is detrapped and travels with continuously decreasing mass whereas the other is stably trapped in its potential well. An extensive list of interaction scenarios, including solitons of different masses, can be considered, and these scenarios can be very interesting in terms of light control applications. It is worth emphasizing that it is the fulfillment of the dynamic power balance condition between the refractive index and the gain-loss profiles that allows for stable soliton dynamics and mutual interactions, which could not take place otherwise.

III. CONCLUSIONS

The fundamental problem of power balance of a nonlinear wave in a photonic structure with unbalanced gain and loss has been addressed. Sufficient conditions between the refractive index and gain-loss profiles have been derived for the dynamic power balance of soliton propagation. In contrast to a static power balance, which ensures only the existence of a fixed

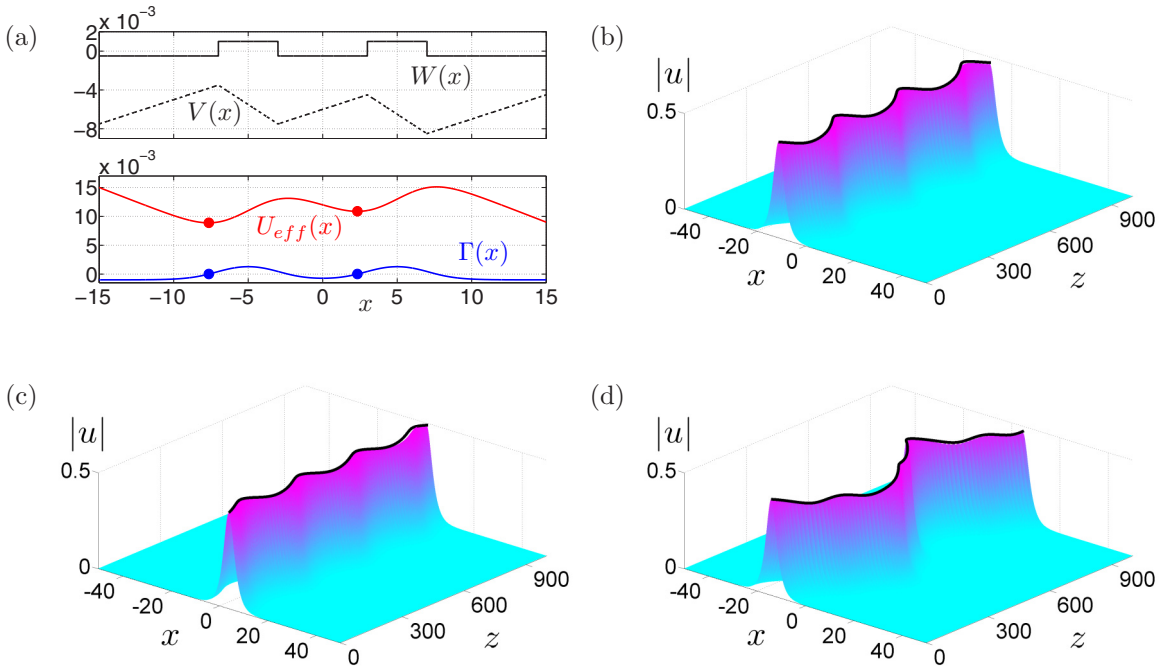

FIG. 3. (Color online) Double hot-spot structure consisted of two amplifying parts ($a_2 = a_4 = 0.001$) of finite width $\Delta x = 4$ located at $x_c = \pm 5$ in a lossy medium ($a_1 = a_3 = a_5 - 0.0005$) for a refractive index profile fulfilling the condition (6) with $C = -1$ ($c_i = -a_i, i = 1,2$). (a) Gain-loss $W(x)$ and refractive index $V(x)$ profiles (top); effective potential $U_{\text{eff}}(x_0)$ and mass variation rate $\Gamma(x_0)$ for a soliton of mass $m = 1$ (bottom). (b) Trapped soliton oscillations in the left potential well for initial position $x_0 = -11$. (c) Trapped soliton oscillations in the right potential well for initial position $x_0 = 4$. (d) Extended trapped soliton oscillations for initial position $x_0 = -14$. The thick black lines depict results from the effective particle model.

point corresponding to stationary soliton propagation, the dynamic power balance ensures the stability of the fixed point solution, allowing for stable propagation for a wide range of initial soliton positions and velocities, which is crucial for realistic applications. The analysis has been based on a simple effective particle model providing not only the sufficient conditions but also an intuitive understanding of the complex soliton dynamics and being in remarkable agreement with the full model. The concepts and results of the dynamic power balance, illustrated here for simplicity only for piecewise constant gain-loss profiles, are so general that they can be directly applied to any type of gain-loss profiles, nonlinear refractive index, and nonlinear gain-loss inhomogeneities, so that the respective conditions can be used as guidelines for the design of realistic photonic structures. Moreover, the consequences of such a dynamic power balance can be considered for the propagation dynamics of different types of waves such as dark and gray solitons as well as two-dimensional solitary wave structures and vortices.

ACKNOWLEDGMENTS

This work has been partially supported by the Research Project NWDCCPS implemented within the framework of the Action "Supporting Postdoctoral Researchers" of the Operational Program "Education and Lifelong Learning" (Actions Beneficiary: General Secretariat for Research and Technology), and it is co-financed by the European Social Fund (ESF) and the Greek State.

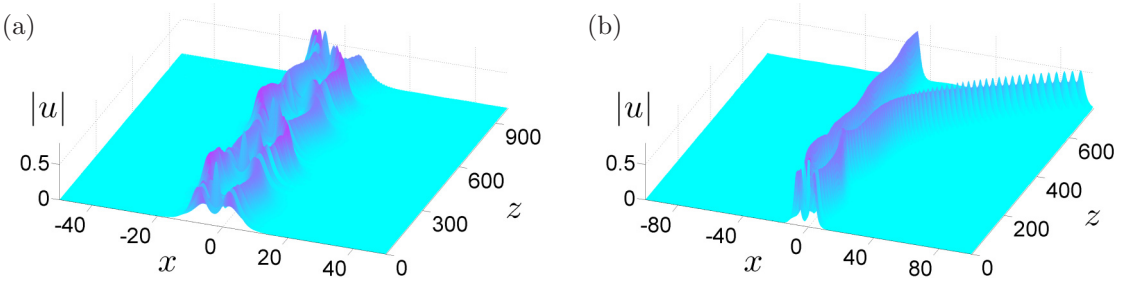

FIG. 4. (Color online) (a) Oscillatory interaction of two solitons of mass $m = 1$ and initial positions $x_0 = -7.65$ and 2.33 corresponding to the two fixed points depicted in Fig. 3(a). (b) Interaction of two solitons of mass $m = 1.5$ and initial positions $x_0 = -7.46$ and 2.54 corresponding to the respective fixed points; the left soliton remains trapped whereas the right soliton is detrapped.

[1] N. I. Zheludev and Y. S. Kivshar, From metamaterials to metadevices, Nat. Mater. **11**, 917 (2012).

[2] A. E. Minovich *et al.*, Functional and nonlinear optical metasurfaces, Laser Photon. Rev. **9**, 195 (2015).

[3] M. Kauranen and A. V. Zayats, Nonlinear plasmonics, Nat. Photon. **6**, 737 (2012).

[4] H. Zhang *et al.*, Z-scan measurement of the nonlinear refractive index of graphene, Opt. Lett. **37**, 1856 (2012).

[5] A. D. Boardman, G. S. Cooper, A. A. Maradudin, and T. P. Shen, Surface-polariton solitons, Phys. Rev. B **34**, 8273 (1986).

[6] E. Feigenbaum and M. Orenstein, Plasmon-soliton, Opt. Lett. **32**, 674 (2007).

[7] A. Auditore *et al.*, Graphene sustained nonlinear modes in dielectric waveguides, Opt. Lett. **38**, 631 (2013).

[8] Y. V. Bludov, D. A. Smirnova, Y. S. Kivshar, N. M. R. Peres, and M. I. Vasilevskiy, Discrete solitons in graphene metamaterials, Phys. Rev. B **91**, 045424 (2015).

[9] P. Tassin, T. Koschny, M. Kafesaki, and C. M. Soukoulis, A comparison of graphene, superconductors and metals as conductors for metamaterials and plasmonics, Nat. Photon. **6**, 259 (2012).

[10] M. A. Noginov, G. Zhu, M. Mayy, B. A. Ritzo, N. Noginova, and V. A. Podolskiy, Stimulated Emission of Surface Plasmon Polaritons, Phys. Rev. Lett. **101**, 226806 (2008).

[11] R. S. Savelev, I. V. Shadrivov, P. A. Belov, N. N. Rosanov, S. V. Fedorov, A. A. Sukhorukov, and Y. S. Kivshar, Loss compensation in metal-dielectric layered materials, Phys. Rev. B **87**, 115139 (2013).

[12] A. Marini, S. Roy, A. Kumar, and F. Biancalana, Loss-compensated nonlinear modes and symmetry breaking in amplifying metal-dielectric-metal plasmonic couplers, Phys. Rev. A **91**, 043815 (2015).

[13] P. Grelu and N. Akhmediev, Dissipative solitons for mode-locked lasers, Nat. Photon. **6**, 84 (2012).

[14] Y. Kominis, S. Droulias, P. Papagiannis, and K. Hizanidis, Gain-controlled dissipative soliton routing in optical lattices, Phys. Rev. A **85**, 063801 (2012).

[15] Y. Kominis, P. Papagiannis, and S. Droulias, Dissipative soliton acceleration in nonlinear optical lattices, Opt. Express **20**, 18165 (2012).

[16] *Spatial Solitons*, edited by S. Trillo and W. Torruellas (Springer, Berlin, 2001).

[17] Y. S. Kivshar and G. P. Agrawal, *Optical Solitons* (Academic, Amsterdam, 2003).

[18] Y. He and D. Mihalache, Lattice solitons in optical media described by the Ginzburg-Landau model with $\mathcal{PT}$-symmetric periodic potentials, Phys. Rev. A **87**, 013812 (2013).

[19] Y. Kominis, Soliton dynamics in symmetric and non-symmetric complex potentials, Opt. Commun. **334**, 265 (2015).

[20] Z. H. Musslimani, K. G. Makris, R. El-Ganainy, and D. N. Christodoulides, Optical Solitons in PT Periodic Potentials, Phys. Rev. Lett. **100**, 030402 (2008).

[21] C. E. Rüter *et al.*, Observation of parity-time symmetry in optics, Nat. Phys. **6**, 192 (2010).

[22] E. N. Tsoy, I. M. Allayarov, and F. Kh. Abdullaev, Stable localized modes in asymmetric waveguides with gain and loss, Opt. Lett. **39**, 4215 (2014).

[23] V. V. Konotop and D. A. Zezyulin, Families of stationary modes in complex potentials, Opt. Lett. **39**, 5535 (2014).

[24] C.-K. Lam, B. A. Malomed, K. W. Chow, and P. K. A. Wai, Spatial solitons supported by localized gain in nonlinear optical waveguides, Eur. Phys. J. Spec. Top. **173**, 233 (2009).

[25] C. H. Tsang, B. A. Malomed, C. K. Lam, and K. W. Chow, Solitons pinned to hot spots, Eur. Phys. J. D **59**, 81 (2010).

[26] C. H. Tsang, B. A. Malomed, and K. W. Chow, Multistable dissipative structures pinned to dual hot spots, Phys. Rev. E **84**, 066609 (2011).

[27] Y. V. Kartashov, V. V. Konotop, V. A. Vysloukh, and L. Torner, Dissipative defect modes in periodic structures, Opt. Lett. **35**, 1638 (2010).

[28] Y. V. Kartashov, V. V. Konotop, V. A. Vysloukh, and L. Torner, Vortex lattice solitons supported by localized gain, Opt. Lett. **35**, 3177 (2010).

[29] D. A. Zezyulin, Y. V. Kartashov, and V. V. Konotop, Solitons in a medium with linear dissipation and localized gain, Opt. Lett. **36**, 1200 (2011).

[30] B. A. Malomed, E. Ding, K. W. Chow, and S. K. Lai, Pinned modes in lossy lattices with local gain and nonlinearity, Phys. Rev. E **86**, 036608 (2012).

[31] E. N. Tsoy, S. Sh. Tadjimuratov, and F. Kh. Abdullaev, Beam propagation in gain-loss waveguides, Opt. Commun. **285**, 3441 (2012).

[32] O. Maor, N. Dror, and B. A. Malomed, Holding the spatial solitons in a pumped cavity with the help of nonlinear potentials, Opt. Lett. **38**, 5454 (2013).